Molecular dynamics of rigid rod polymers

B. L. Farmer* and B. R. Chapman
Department of Materials Science, University of Virginia, Charlottesville, VA 22903-2442, USA

and D. S. Dudis† and W. W. Adams‡
Wright Laboratory, Materials Directorate, †WL/MLBP and ‡WL/MLPJ, Wright-Patterson Air Force Base, OH 45433-6533, USA
(Received 24 February 1991; revised 20 May 1992)

Molecular dynamics (MD) calculations have been used to study the behaviour of isolated rigid rod molecules of poly(*p*-phenylene), poly(*p*-phenylene benzobisthiazole) and poly(*p*-phenylene benzobisoxazole). The molecular mechanics force field was initially modified to improve agreement between minimized structural geometries and available X-ray data, as well as results from semiempirical molecular orbital calculations. The MD simulations show the molecules to be surprisingly flexible, with changes in end-to-end distances as large as 16%. An examination of the energies (calculated by various methods) associated with out-of-plane bending deformation, suggests that the rigid rod polymers may in fact be even more flexible than the simulations indicate. The results provide rationalizations for the relatively short persistence lengths measured in solution and for bending observed in high-resolution electron micrographs of these materials.

(Keywords: molecular dynamics; rigid rod polymers; polyphenylene; PBO; PBZT; PPP; persistence length)

INTRODUCTION

Rigid rod polymers have received much attention[1,2] because of their high mechanical properties, thermal/oxidative stability, environmental resistance, and more recently, their third-order non-linear optical properties[3–9]. Of particular interest have been poly(*p*-phenylene benzobisthiazole) (PBZT) and poly(*p*-phenylene benzobisoxazole) (PBO) which have been studied as alternatives to carbon and aramid fibres in composites, and poly(*p*-phenylene) (PPP) which has been studied as the prototypical rigid rod polymer and because of its electrical conductivity. The remarkable material properties of these polymers arise, in part, from the high degrees of molecular orientation that can be obtained in fibres spun from lyotropic liquid-crystalline solutions[10,11]. Further, their molecular structures, consisting of aromatic rings joined together through *para* linkages, suggest that their high strength at the molecular level[12,13] might be expressed even at the macroscopic level without the intervention and attenuation of morphologies such as chain folding and other defects.

The most straightforward (but perhaps naive) picture that might be developed of rigid rod polymers would be molecules behaving in a stiff, pencil-like fashion or as uncooked spaghetti. To the extent that the bonds joining the rings are collinear (which they nearly are in the minimum energy structures), conformational rotations about those bonds would be ineffectual in changing the trajectory of the molecule. At odds with this simple picture are two experimental observations.

Light-scattering measurements on solutions of rigid rods suggest persistence lengths in the range of a few hundred angstroms. The observed lengths[14,15] ($\sim$500–650 Å) are considerably shorter than the actual contour lengths[16] ($\sim$1200–1500 Å) of the supposed rods, based on their molecular weights. Although the experimental measurements of persistence length are complicated by the effects of aggregation, such effects would tend to overestimate the stiffness, so that the actual persistence of the individual rods may be even smaller than the reported measurements. Although far from the common polymer coil with its very small persistence length, the rigid rod polymers appear to be more flexible than might be surmised from their lack of conformational flexibility.

The second experimental observation that calls for reassessing the pencil-like model is from high-resolution transmission electron microscopy of the polymers in the solid state[17]. After being subjected to compressive stresses, the molecules within kink bands apparently bend in a cooperative manner. Changes in chain axis direction of 38° over distances of 0.5 nm are observed in PBO. From the simple viewpoint, this surprisingly dramatic bending might be attributed to breaking molecules. Alternatively, the molecules may have some heretofore unanticipated (or unappreciated) deformation mechanism to allow such bending without bond rupture.

This paper reports the results of molecular dynamics (MD) simulations undertaken to explore the nature of molecular flexibility of isolated PBO, PBZT and PPP molecules. The preliminary results of MD simulations of molecules embedded in a crystalline array have also been reported[18]. MD extends the technique of molecular mechanics[19] to encompass the exploration of time- and temperature-dependent molecular processes. It uses the same force field and geometric description of the molecule as does molecular mechanics. Several books and articles present detailed treatments of the methods[20–22]. In simple terms, the MD calculations proceed as follows. First, the force acting on each atom is computed from the bond stretches, angle bends, torsions and van der

* To whom correspondence should be addressed

0032-3861/93/081588-14

Waals interactions associated with the (momentary and transitory) geometry of the molecule. From this force and Newton's Law, the acceleration of each atom is computed and assumed to act for a short time interval (typically of the order of 1 fs). The velocities, thus calculated, are scaled to the specified temperature of the simulation using

$$3Nk_BT = \sum m_i v_i^2 \quad (1)$$

where T is the absolute temperature, k_B is Boltzmann's constant, m_i and v_i are the mass and velocity of the ith atom and N is the total number of atoms. These scaled velocities, acting for a short time, bring the atoms to new positions and modify the forces which they experience. The forces are once again evaluated and the procedure is repeated until the simulation has accumulated a specified number of time steps.

METHODS

The calculations were made using the SYBYL[23] molecular modelling package. Molecular mechanical energy minimizations and MD studies were carried out entirely within SYBYL. In addition, SYBYL served as the interface to the MOPAC molecular orbital program, allowing utilization of its graphical display capabilities. The same force field was used for both molecular mechanics and dynamics calculations. The parameters were those of the Tripos force field[24], modified (as described below) to provide better agreement with the results of molecular orbital calculations and with the results of X-ray structure analyses of PBZT and PBO[25], on model compounds for PBZT[26] and on related polymers[27].

The dynamics program uses the Verlet (or leap frog) method[28] to calculate atom velocities and positions at alternate half time steps. Time steps of 1 fs were used. Initial runs lasted for 2500 fs. Longer runs (35 000 fs) were also carried out to be certain start-up effects had been eliminated. Atomic positions and velocities were stored and most data analysis was carried out by considering data at 50 fs intervals. The MD simulations began with a warm-up period consisting of 50 fs time intervals at 50, 100, 150, 200 and 250 K, followed by 2500, 5000, 15 000 or 35 000 fs at the desired temperature of 300 K. Momenta were reset and the non-bonded interaction list was updated every 25 fs. The temperature-coupling factor[23], a parameter used to impose gradual rather than abrupt temperature changes (akin to a proportional temperature controller), was 10. All atoms were considered explicitly. The Shake algorithm[29], which can be used to eliminate consideration of C—H stretching vibrations and allow larger time increments, was not employed. Electrostatic contributions to the energy were not considered. In reality, the partial charges are likely to depend upon the torsion angles between rings. Since the MD software has no means of considering conformationally dependent charges, and because of uncertainties associated with the appropriate means of dealing with the dielectric constant, it was felt that including electrostatic interactions would perhaps introduce more error than would neglecting their effects. The simulations were performed without solvent or periodic boundary conditions, and therefore represent the molecules as they might exist and behave *in vacuo*.

The *cis* form of PBO and the *trans* form of PBZT were studied. MD calculations were made on chain segments that were ~50 Å in length. For PBO and PBZT, this corresponds to five repeat units, and for PPP, 14 phenyl rings. To investigate the effect of chain length, chains of PBO and PBZT having seven repeat units were also considered. In each case, alternate rings down the chain were initially coplanar. The starting torsion angles about the backbone single bonds were 45° in PPP, 20° in PBZT and 1° in PBO. This latter value was chosen (rather than the minimum energy 0° value) to avoid a prolonged induction time before the molecule began to undergo normal dynamic motions. The starting conformation for PBZT had successive heterocycles all oriented in the same direction, while the starting conformation for PBO had successive heterocycles alternating 180° in orientation. The starting geometries were those that resulted from a molecular mechanics minimization of one repeat unit. The repeat units were then connected so that the inter-unit single bond had the same length as the intra-unit single bond.

Force field

The molecular mechanics calculations on PBO and PBZT previously reported[30] used the Chem-X molecular modelling software[31] and the accompanying force field. The parameters describing the torsional energy barriers for the inter-ring single bonds were adjusted to produce agreement with results of semiempirical molecular orbital calculations using the AM1[32] Hamiltonian in MOPAC[33]. Since the present calculations used the Tripos force field and parameters[24] and the SYBYL modelling software[23], it was necessary to re-examine and adjust the torsional potential to provide agreement with AM1 results. Additional modifications were also made to obtain better agreement with the molecular geometries determined for model compounds by X-ray structure analysis[25–27]. *Figure 1* shows the repeat units of PBZT and PBO.

Modifications to the force field were made by adjusting the selected parameters listed in *Table 1*. After each parameter change, the geometry was optimized with the

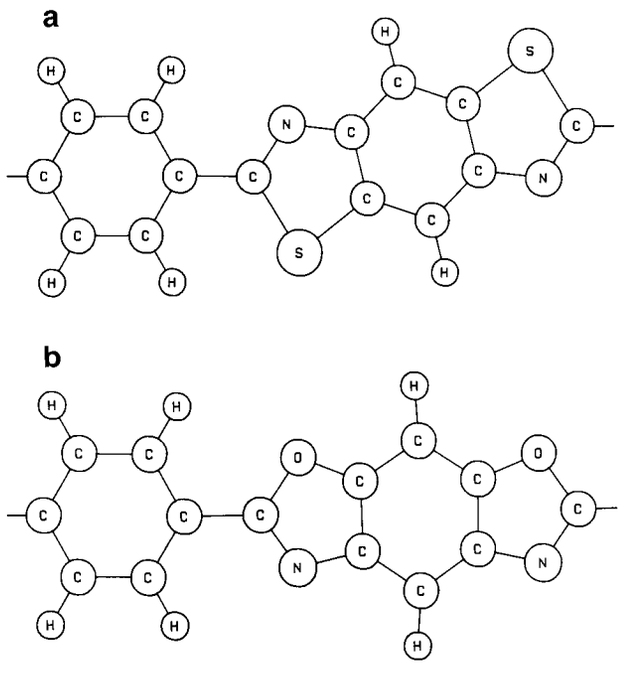

Figure 1 Schematic diagrams of (a) *trans*-PBZT and (b) *cis*-PBO

Table 1 Modified energy parameters[a]

		Force constant[b]	Equilibrium value
PBZT			
Torsion	$*—C_2—C_{ar}—*$ (single bond)	0.43	
Angle bend	$*—S—*$	0.03	100°
	$C_2—N—C_{ar}$	0.08	118°
Bond stretch	$C_2—C_{ar}$ (single bond)	1000	1.48 Å
PBO			
Torsion	$*—C_2—C_{ar}—*$ (single bond)	0.72	
Angle bend	$C_2—N—C_{ar}$	0.08	118°
Bond stretch	$C_2—C_{ar}$ (single bond)	1000	1.48 Å
PPP			
Torsion	$*—C_2—C_{ar}—*$ (single bond)	1.00	
Angle bend	$C_{ar}—C_{ar}—H$	0.002	120°
Bond stretch	$C_2—C_{ar}$ (single bond)	633.5	1.48 Å

[a] * Denotes an atom of any type; C_{ar} denotes an aromatic carbon; C_2 denotes an sp^2 carbon

[b] Units of force constants are as follows: bond stretch, kcal (mol-Å)$^{-1}$; angle bend and torsion, kcal (mol-deg)$^{-1}$

molecule constrained at each 10° interval of the inter-ring torsion angle, over the range 0–90°. Comparisons were made with selected geometrical parameters from the X-ray structures of the model compounds[25–27], and with torsion energy curves calculated using AM1. The resulting parameters, presented in *Table 1*, gave agreement with observed bond lengths and angles within 5%. This set of parameters will be denoted herein as the tailored Tripos force field.

It was also necessary to optimize the force field for use with PPP. *Figure 2* shows plots of energy (calculated using AM1 and molecular mechanics) *versus* torsion angle for rotation about the inter-ring single bond in biphenyl. The molecular mechanics torsion force constant (primarily) was adjusted systematically until adequate agreement with the AM1 data was achieved. The resulting parameter values are also shown in *Table 1*. *Figure 2* shows the results of the molecular mechanics calculations using the tailored (Tripos) force field and performed in an analogous fashion to the AM1 calculations, i.e. with constrained minimizations carried out at 10° intervals. While the energy minimum is shifted by about 4°, and there appears to be some minimization artefact at 40° in the molecular mechanics results, overall the character of the curve adequately mimics the AM1 results. The differences in energies at 0, 45, and 90° are within about 0.1 kcal mol^{-1} of the values calculated by AM1. The torsion energy curves are in reasonable agreement with experimental values[34,35] for the location (40–45°) and depth of the energy minimum (1–2 kcal mol^{-1}). Recent *ab initio* results[36], while still giving the minimum near 45°, find a barrier of 3.5 kcal mol^{-1} at 0° torsion, compared with the AM1 value of 2.2 kcal mol^{-1}. The discrepancy with experimental values was attributed to the assumption of an inappropriate form for the potential function used to extract the barrier heights from the experimental data. Recently, the potential energy curve with respect to the biphenyl torsion has been reassessed[37].

In aromatic rings and similar bonding environments, one contribution to the energy arises from out-of-plane bending, which is based on the deviation of a central atom from the plane defined by the three atoms to which it is bonded[24]. In the present polymers, out-of-plane bending can contribute significantly (as will be seen) to reducing the end-to-end distance of the molecule. This energy contribution is likely to be especially important for the atoms at either end of the backbone single bond and perhaps at the midplane of the heterocycle. The force constant for this deformation (supplied in the original Tripos force field[24]) is 480 kcal (mol-Å)$^{-1}$ for aromatic and sp^2 carbons. It has been noted[23] that this value is too small and leads to unacceptably large deviations from planarity of the minimized structures of model compounds (such as benzene). A value of 630 kcal (mol-Å)$^{-1}$ has been recommended[23] as giving better agreement with crystallographic data. In addition, a torsional force constant of 2.35 kcal (mol-deg)$^{-1}$ for $*—C_{ar}—C_{ar}—C_{ar}$ torsions was added to the force field. (C_{ar} denotes an aromatic carbon and * denotes any type of atom.) Calculations were made with both the original and modified out-of-plane bending parameters. They did not show dramatic differences. The MD results reported here were made using the modified (630 kcal (mol-Å)$^{-1}$) out-of-plane bending parameters.

RESULTS

Static trajectories

It has long been recognized that the geometry of the heterocyclic ring system in PBZT provides a slight non-linearity to the repeat unit of the polymer, i.e. the bonds which connect to the phenyl groups at either end are not collinear. The simplest explanation of the observed relatively short persistence length would be this non-linearity of the repeat unit itself. The extent to which this might contribute to the observed persistence lengths was, thus, first considered. The geometries resulting from energy minimizations, however, had slight atomic displacements out of the planes of the rings. These displacements led to angles measured between the *para* connections across a phenyl ring of 176° instead of the expected 180°. Such deviations were deemed too large to allow meaningful assessment of the deviations from linearity in the static trajectories of the rigid rods. To assure proper geometry of the molecules and to avoid deviations of the type noted above, the following procedure was used. The geometries for each component ring for the several polymers of interest were first optimized using molecular mechanics. This unit was then oriented such that its atoms lay as closely as possible in the *xy* plane, and the *z* coordinate of each atom was set

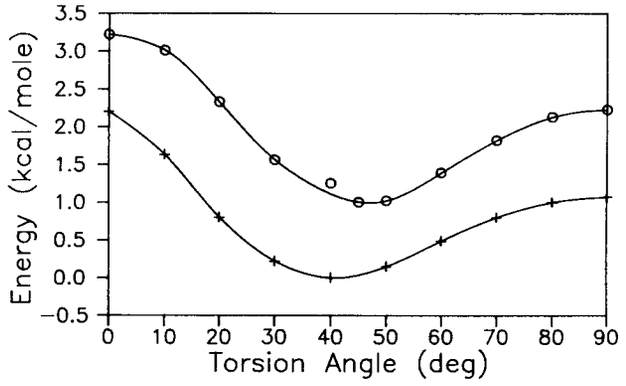

Figure 2 Relative energy *versus* torsion angle for biphenyl calculated using AM1 (+) and molecular mechanics (○). For clarity, molecular mechanics data have been offset by 1 kcal mol^{-1}

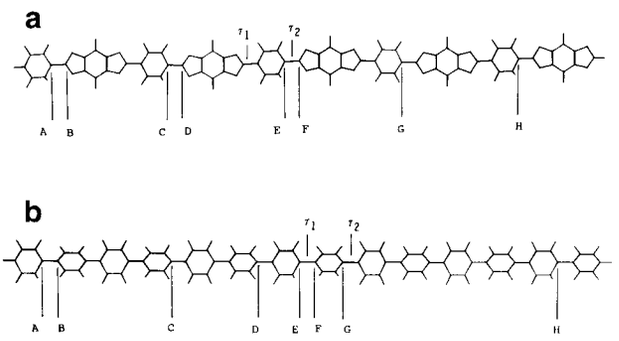

Figure 3 Schematic diagram of models of (a) PBO and (b) PPP showing labels used to characterize molecular trajectories

Table 2 Trajectory data for rigid rod polymers

Polymer		AC (Å)	AE (Å)	∠ACE (deg)	∠ABE (deg)
PPP		12.9	25.7	180.0	180.0
trans-PBZT	*syn*	12.5	25.0	178.8	176.2
	anti	12.5	24.9	170.5	179.4
cis-PBO	*syn*	12.2	24.3	173.9	172.7
	anti	12.2	24.3	178.5	176.7

to zero. The maximum shifts thus imposed were on the order of a few hundredths of an angstrom. These planarized components were then used to construct chain lengths of the order of 25–30 Å, corresponding to three repeat units of PBZT and PBO polymers.

The trajectories of the rigid rod polymers might be characterized in a number of ways. The measurements used here are illustrated in *Figure 3*. For polymers containing the benzobisthiazole and benzobisoxazole heterocycles, distances were measured between the same atom in neighbouring and next-neighbouring repeat units of the polymer. For a linear polymer, the latter value (AE) should be twice the former (AC). Another measure of the linearity is the angle (ACE) between vectors connecting a central atom to equivalent atoms in neighbouring repeat units to either side. Finally, the angle (ABE) between the vector (BA) of the first inter-unit single bond and the vector from the terminus (B) of that bond to atom (E) in the next-neighbouring repeat unit was measured. In PPP measurements were made in an analogous fashion. The labelling for PPP is also shown in *Figure 3*.

The static trajectories are slightly dependent on the orientations of the repeat units. Conformations at the two extremes are listed in *Table 2*. The terms '*syn*' and '*anti*' refer to the relative orientations of the heterocycles, with '*syn*' indicating that the sulfur atoms (or oxygens) in successive repeat units are oriented in the same direction, while '*anti*' indicates opposite orientations. For PBO the torsion angles were 0°, leaving the rings coplanar. For PPP, a torsion angle of 45° was used[36]. For *trans*-PBZT[26], a torsion angle of 30° was used. The sequence of torsion angles was such that the planes of alternating rings along the chain were parallel or coplanar.

The trajectory angles are in the range 170–180°. The slight misorientation (up to 10°) between the bonding directions and the molecular axis may provide a relatively 'soft' deformation mode that would impact the initial axial strain of the polymers and contribute to their non-linear elasticity[38].

The persistence length a for a worm-like chain[39] is given by:

$$a = -\Delta L / \ln \langle \cos \Delta\psi \rangle \qquad (2)$$

where ΔL is the segment length. $\Delta\psi$ is the angle between neighbouring chain segments, and is the supplement of the value given in *Table 2*. For the polymers of interest here, the persistence lengths calculated using this model and the calculated deflection angles are too large in comparison with experimental values. The average deflections for *syn* and *anti* conformers are 177° for PBO and 175° for PBZT. For an infinite chain, these deflections give persistence lengths of 9000 and 3000 Å, respectively. More practically, for realistic molecular weights, the persistence length would be equal to the contour length. For PPP, the persistence length would also equal the contour length since $\Delta\psi = 0°$. Clearly, the trajectories as dictated by static bonding geometry do not account for the experimentally observed persistence lengths, which would require $\Delta\psi$ values of the order of 11–12°.

Molecular dynamics

Figure 4 shows the time–temperature profile for the first 5000 fs of the dynamics run for PBZT, and *Figure 5* shows the kinetic, potential and total energies over this same time interval. *Figure 6* shows plots of the end-to-end distance (AH) and the length of the central repeat unit (EG). *Figure 7* shows the corresponding geometric data from the dynamics simulation of a five-repeat chain of PBO (see *Figure 3* for the atom labelling scheme). The

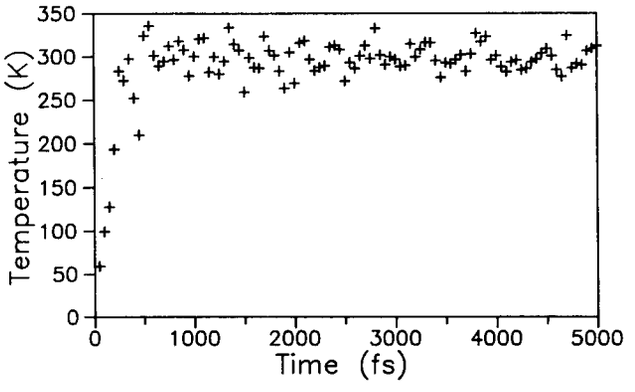

Figure 4 Temperature *versus* time for the MD simulation of PBZT

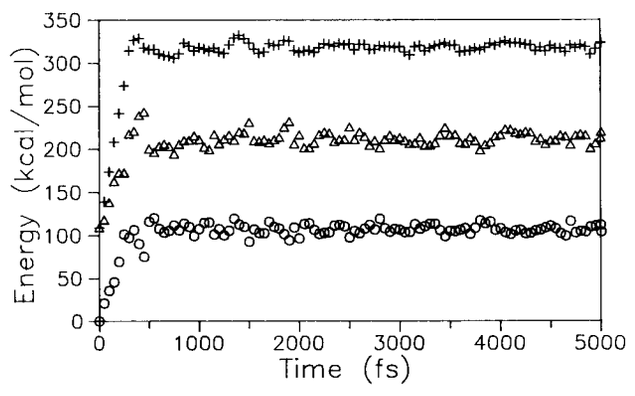

Figure 5 Energies *versus* time for PBZT: (○) kinetic energy, (△) potential energy and (+) total energy

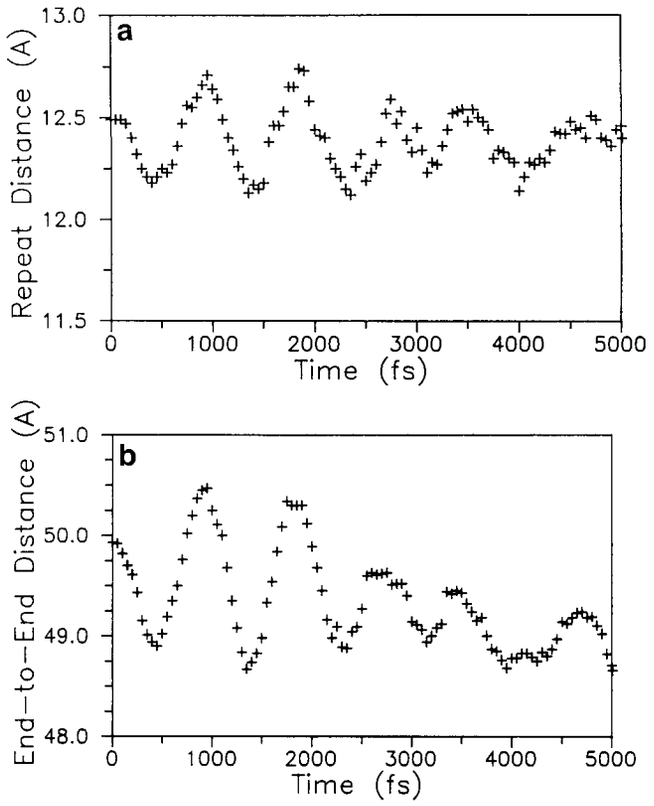

Figure 6 (a) Repeat distance and (b) end-to-end distance *versus* time for PBZT

original out-of-plane bending parameters were used in these simulations.

For both PBO and PBZT, a particularly striking feature of the distance plots is the oscillation as a function of time. The oscillations are reminiscent of those in the total energy *versus* time as seen in simulations of polyethylene[40]. The oscillations persist considerably longer than the equilibration (warm-up) time at the beginning of the simulation. It might be supposed that the oscillations arise from an incorrect starting geometry (perhaps too long or too short), but the starting geometries were in fact minimized using the same force constants as used in the dynamics simulations.

The effects of the out-of-plane bending force field parameters were explored by using the modified out-of-plane bending parameters (discussed above) in a 5000 fs dynamics run. The oscillations are not altered significantly by the revised energy parameters. Their period is unchanged and their amplitude, in fact, may be slightly larger. Similar results were obtained using a time increment of 0.5 fs (instead of 1 fs) for the MD simulations.

To investigate further the nature of the oscillations, simulations (5000 fs) were also performed with a PBZT oligomer containing seven repeat units. Measurements of distances or angles associated with one, five or seven units of this chain all showed the same periodicity. However, the periodicity of five units of this seven-repeat chain was different from the periodicity measured in simulations on the five-repeat oligomer, as shown in *Figure 8*. In this short time interval, where the molecules are still fairly linear, the period and the amplitude of the oscillations increase as chain length increases.

To determine if the oscillations might be characteristic only of the early-time portion of the dynamics, 35 000 fs runs were also carried out using both original and modified out-of-plane bending parameters. Both force fields gave similar results. The end-to-end distance data are shown in *Figures 9a–c*, for PBO, PBZT and PPP, respectively, using the modified parameters. Although other effects come into play, the high frequency oscillations clearly persist even to the longest simulation times.

Figure 10 shows the Fourier transforms[41] of the end-to-end distance *versus* time data for the initial 5000 fs of the simulations shown in *Figure 9*. For PBO, PBZT and PPP, the oscillations of interest (corresponding to the largest peaks in the transforms) have frequencies of 1304, 1121 and 1006 GHz and periods of 767, 892 and

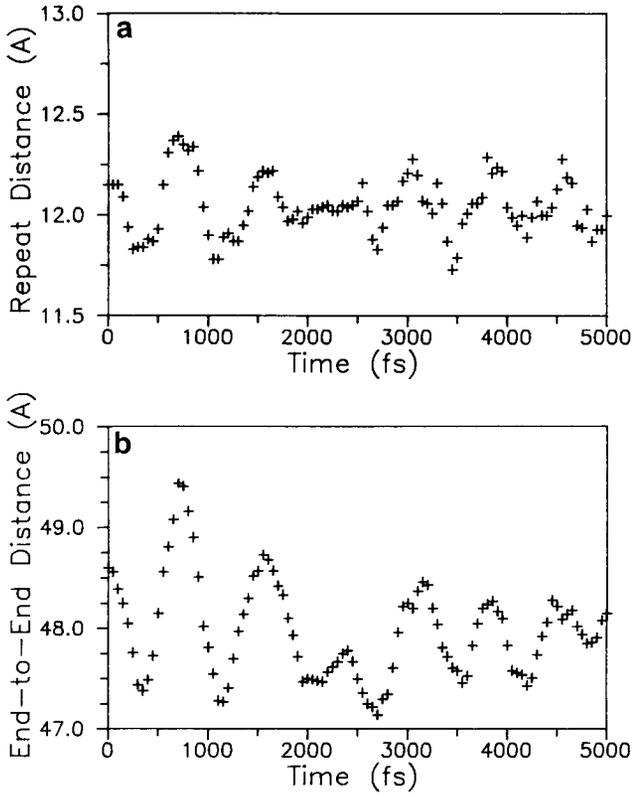

Figure 7 (a) Repeat distance and (b) end-to-end distance *versus* time for PBO

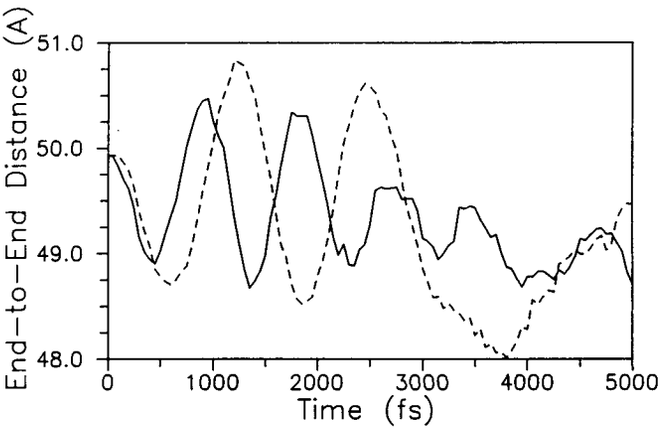

Figure 8 Comparison of end-to-end distance *versus* time data for five-repeat molecule (——) and central five units of seven-repeat molecule (– – –)

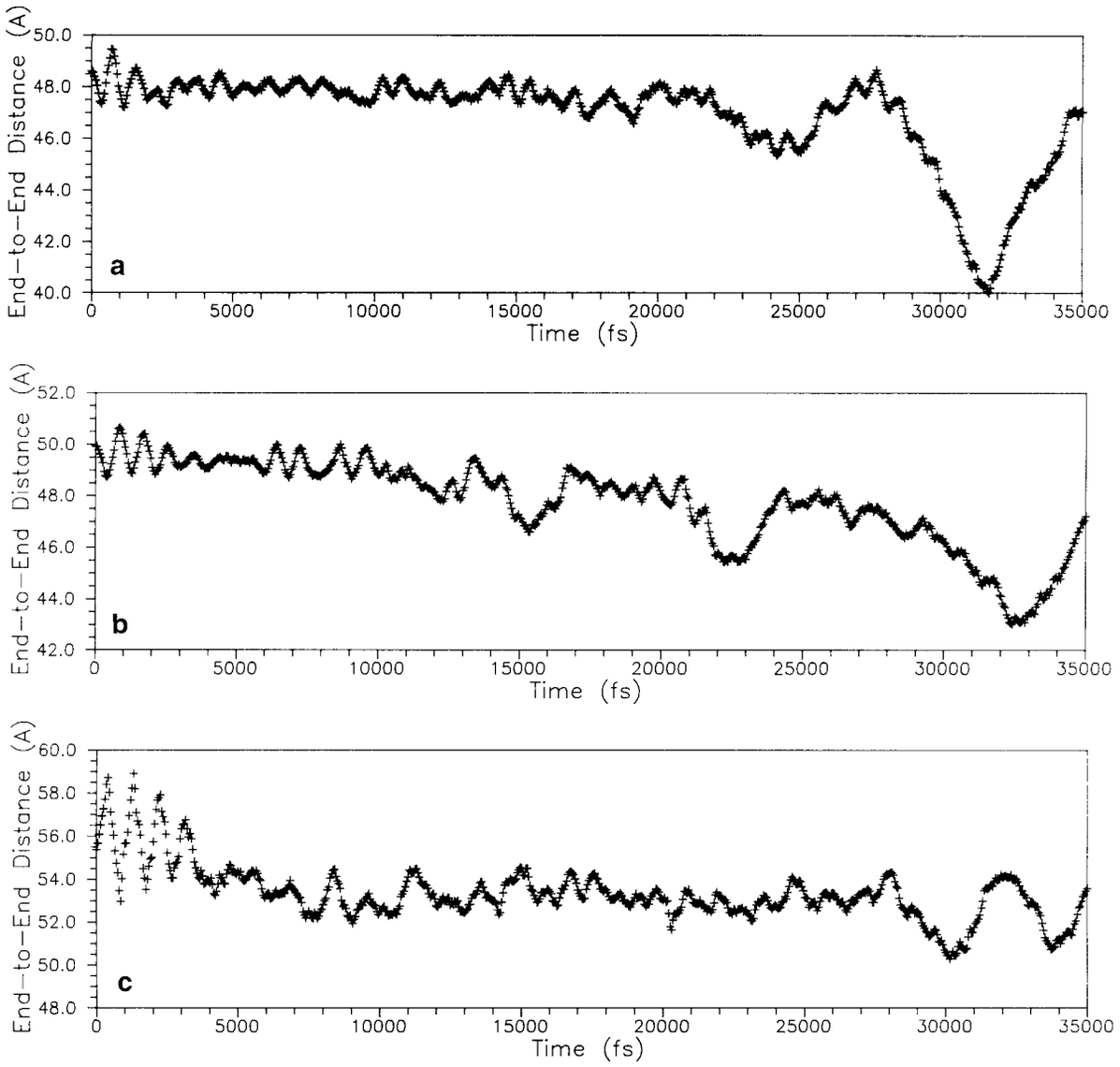

Figure 9 Repeat distance *versus* time for extended MD simulations for (a) PBO, (b) PBZT and (c) PPP

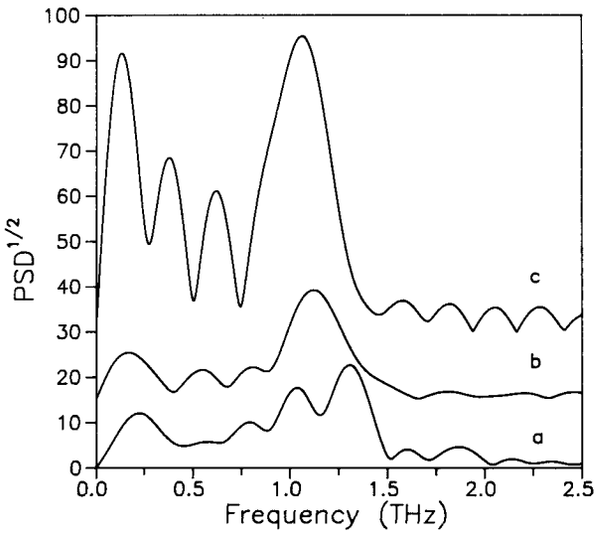

Figure 10 Fourier transforms of the initial (5000 fs) end-to-end distance *versus* time data for (a) PBO, (b) PBZT and (c) PPP. The PBZT and PPP curves have been vertically offset by 15 and 30 units, respectively

994 fs, respectively. It is interesting to note that this ordering of the polymers by increasing period correlates with the relative moduli of the materials. Assuming the polymer segment approximates a circular rod and that its oscillation frequency corresponds to a fundamental longitudinal vibration frequency, the modulus of the rod can be calculated from the relation[42]:

$$f = 0.5\pi^{1/2} r (E/m)^{1/2} L^{-1/2} \quad (3)$$

where f is the fundamental vibrational frequency, r and L are the radius and length of the cylinder, E is its modulus and m is its mass. The values of the modulus thus computed are shown in *Table 3*. The values are roughly a factor of 2 smaller than the theoretical moduli calculated by the AM1 method[12,13] and using the crystallographic cross-sectional area. If this discrepancy is attributed to assumptions made in the analysis, even this order of magnitude agreement suggests that the oscillations relate to the fundamental properties of the rigid rod molecules, and that Fourier transformation of such data may provide valuable insight into the properties of such materials. Note also that the increased

Table 3 Calculated dynamic moduli

Polymer	r (Å)	L (Å)	f (THz)	m (10^{-21} g)	E (GPa)	AM1[a] (GPa)
PPP	2.5	60.7	1.01	1.77	220	450
PBO	2.5	61.4	1.31	1.94	410	730
PBZT	2.5	63.1	1.12	2.21	360	610

[a] From ref. 13

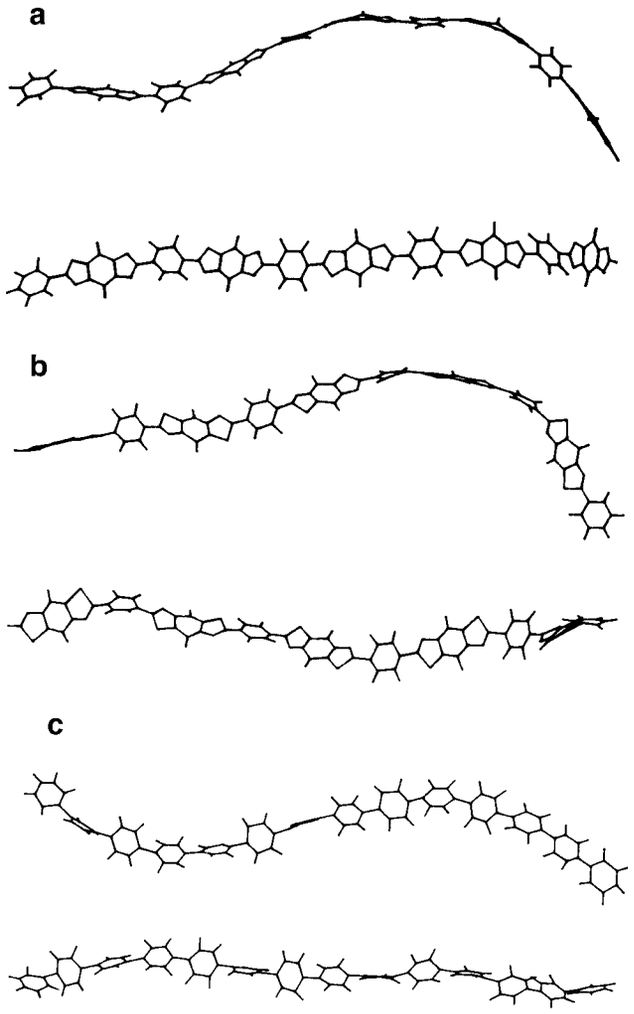

Figure 11 Orthogonal views of the molecular trajectories of (a) PBO, (b) PBZT and (c) PPP during the MD simulations

period (frequency^{-1}) observed in the simulations of the seven-unit oligomer is quantitatively consistent with increasing the mass and length in equation (3). Alternatively, the factor of 2 discrepancy could be attributed to the possibility that the molecular mechanics force field simply describes the molecule as less stiff than does the AM1 method. In fact, calculations for a PPP chain using the tailored MM force field and evaluating the energy at a sequence of static elongations, yields a modulus of 280 GPa. Thus, the factor of 2 discrepancy seems more attributable to discrepancies in the force field than to the method of extracting the modulus (MD or MM). Presuming the AM1 approach yields a more valid estimation of the actual molecular properties, modifications to the molecular mechanics force field would be in order.

The oscillations in the end-to-end distance with time suggest a fundamental flexibility in these rigid rod polymers[18]. Solvent molecules may influence the details of the oscillations, but not this inherent flexibility, except perhaps when the solvent causes chemical changes in the polymer, such as protonation in a strong acid solvent. Importantly, the oscillations imply that a rigid rod molecule would seldom be completely straight. The compressive properties of even a slightly bent molecule would be expected to be dramatically lower than one in which such stresses could be applied exactly coaxial with the covalent bonding of the molecule.

The magnitudes of the changes in the end-to-end distance are surprising. Even in the 5000 fs data, the 1.5 Å length changes in PBZT, and 2.5 Å changes in PBO, are quite remarkable (for molecules 50 Å long) for what have been envisioned to be very stiff molecules. More surprising still are the tremendous fluctuations seen in the 35 000 fs data shown in *Figure 9*. These changes amount to 16, 14 and 11% decreases in end-to-end length for PBO, PBZT and PPP, respectively. The distances are no longer representative of a linear, extended molecule. Rather, the molecules have developed substantial (transitory) bends, as shown in *Figure 11* which shows the PBO, PBZT and PPP molecules at times near those corresponding to their respective shortest end-to-end distances. Calculations using the original and modified out-of-plane bending parameters did not differ dramatically in the magnitudes of these fluctuations.

Much of the deformation that leads to the non-linear molecular trajectories can be characterized as out-of-plane bending, occurring primarily at the atoms at either end of the backbone single bond and perhaps at the midplane of the heterocycle. A simple depiction of this type of deformation is shown in *Figure 12*, which shows superimposed side views of a PBO repeat unit with bend angles of 0, 5, 10 and 15°. Both bond angle and out-of-plane bending energies would contribute to the total energy associated with such deformation. *Table 4* shows the various contributions to the energy for the starting PBO structure (minimized but with the torsion angle set to 1°) and the structure from the dynamics run shown in *Figure 11*, which shows considerable deviation from linearity. Also shown is the energy for this same

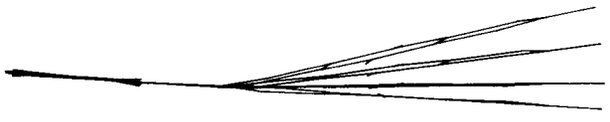

Figure 12 Side view of PBO repeat unit showing bending deformation at the heterocycle carbon atom

Table 4 Energy contributions (kcal mol^{-1})

	Initial	Dynamics	
		Original FF	Revised FF
Bond stretching	12.3	55.2	55.2
Angle bending	161.8	189.2	189.2
Torsion	0.0	15.5	26.5
Out-of-plane	0.0	14.2	17.8
1–4 van der Waals	3.8	4.8	4.8
Van der Waals	−9.9	−10.5	−10.5
Total potential energy	168.0	268.4	283.0

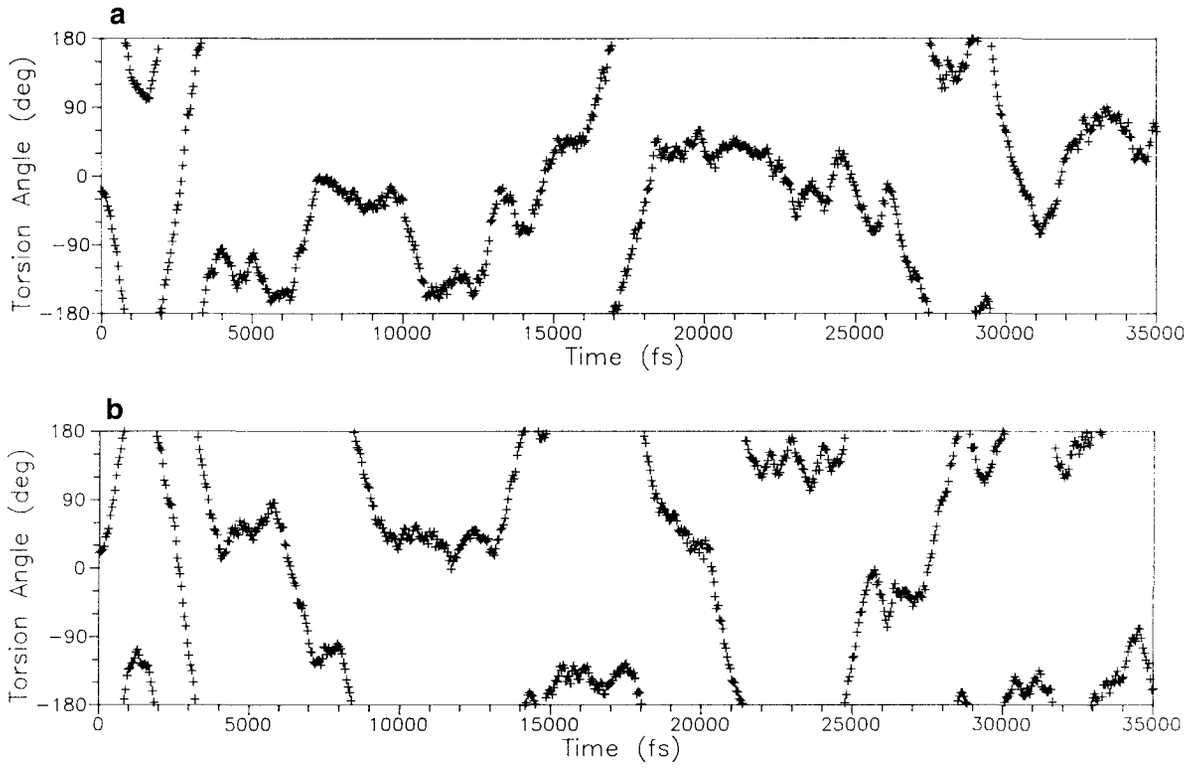

Figure 13 Torsion angles (a) $\tau 1$ and (b) $\tau 2$ *versus* time for PBZT

structure computed with the revised parameters for out-of-plane bending. The angle bending, bond stretching and torsion energy for the dynamics structure are each considerably larger than those of the minimized structure. The out-of-plane bending contribution is increased by only 14 kcal mol^{-1} using the original parameters, and only by 18 kcal mol^{-1} using the modified parameters. Non-bonded interactions change by fairly small amounts. While all types of bonding deformations contribute to the overall shape of the molecule, the out-of-plane bending deformation results in disproportionately large deviations of the molecule from linearity. The validity of the force constants pertaining to this out-of-plane bending are thus especially important and will be examined further.

In a straight rigid rod polymer chain (as shown in *Figure 3*), rotations about the backbone single bonds do not significantly affect the trajectory of the molecule, because the bonds are nearly collinear with the molecular axis. As soon as the molecule becomes non-linear (by out-of-plane bending), these torsional rotations become a significant factor in determining the overall trajectory. As an example, if the torsion angles were all 0° (all rings coplanar), out-of-plane bending would allow the molecule only two-dimensional freedom, in a plane normal to that containing the rings. At other torsion angles, the molecular trajectory can take on three-dimensional character. More important is the converse, namely, that at other torsion angles, out-of-plane bending is likely to be an even easier mode of deformation, because the *ortho* hydrogens on the phenyl rings will be less of an impediment to such bending.

Figures 13 and *14* show for PBZT and PBO, respectively, the torsion angles to either side of the central phenyl group. While PBO shows a tendency to oscillate about values of 0 and 180° for extended periods, PBZT tends to be less resident at any particular torsion angle. Excursions through torsion angles of +90° or −90° are indicative of flips of the phenyl ring with respect to its neighbouring heterocycles. The number of such flips in PBZT is about one-third greater than in PBO, reflecting the difference in the torsional energy barriers for PBZT (1.60 kcal mol^{-1}) *versus* PBO (2.56 kcal mol^{-1}). Transitions through ±90° in one torsional angle seem often to be accompanied by a subsequent transition in the other torsion angle, indicating that the phenyl ring often rotates with respect to both its neighbouring heterocycles. Occasionally, however, flips do occur with respect to only one neighbouring heterocycle. This cannot, however, be construed as one end of the molecule spinning with respect to the other, since only the second neighbouring heterocycle may be following along and not the rest of the chain.

Figure 15 shows scatter plots of these same torsion angles in PBZT and PBO. Clustering of points indicates a tendency for the torsion angles to be coupled. There is indeed some clustering present, and apparently slightly more so in PBO than in PBZT. In PBZT, the clustering appears to be displaced from coplanar values (0 and 180°), as would be expected from its torsion energy curve. Further analysis of the coupling of ring rotations, and the correlations of ring orientations is presently underway. In addition, AM1 calculations[43] indicate that coordinated rotations along the chain may be energetically advantageous.

Figure 16 shows the torsion angles to either side of the central ring in the PPP molecule. The torsion angles show constant oscillation about 45° (or its energetic equivalents at −45, 135, or −135°), with occasional transitions over the barrier at 90° into the other (135°) low-energy region. The resulting average torsion angle of about 90° shown in these simulations may have implications for the experimental determinations of the

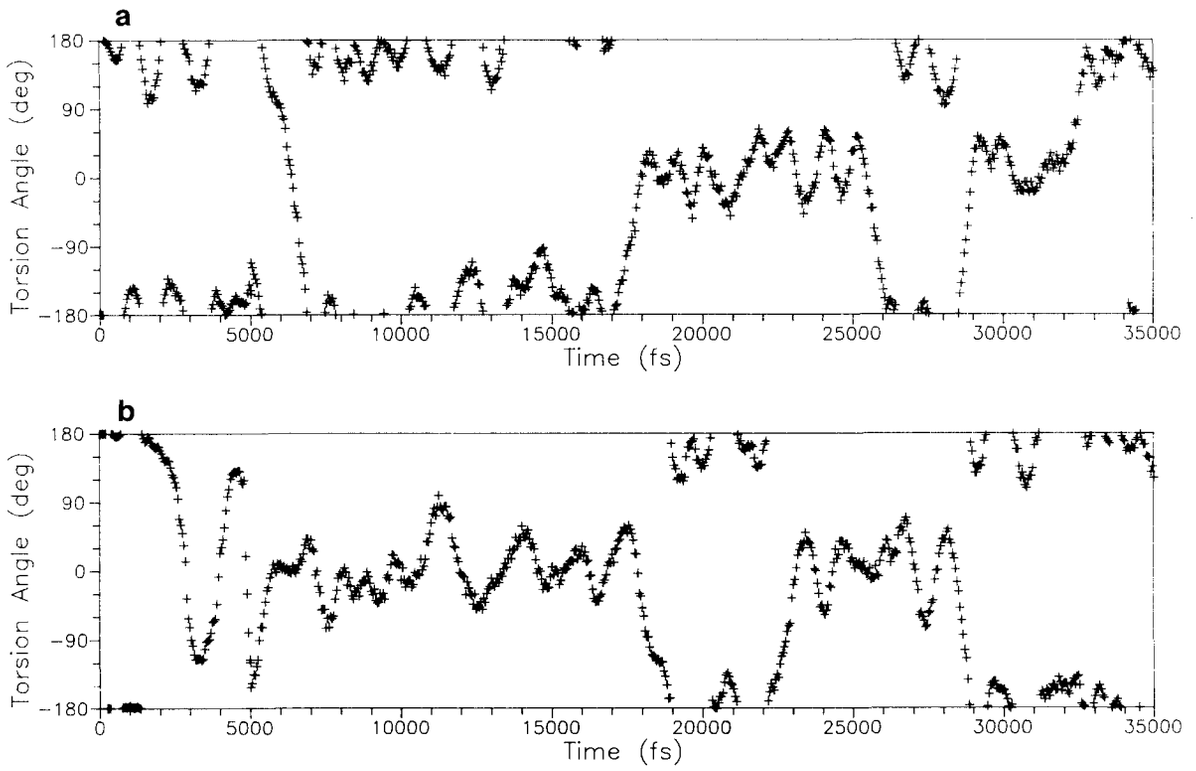

Figure 14 Torsion angles (a) $\tau 1$ and (b) $\tau 2$ *versus* time for PBO

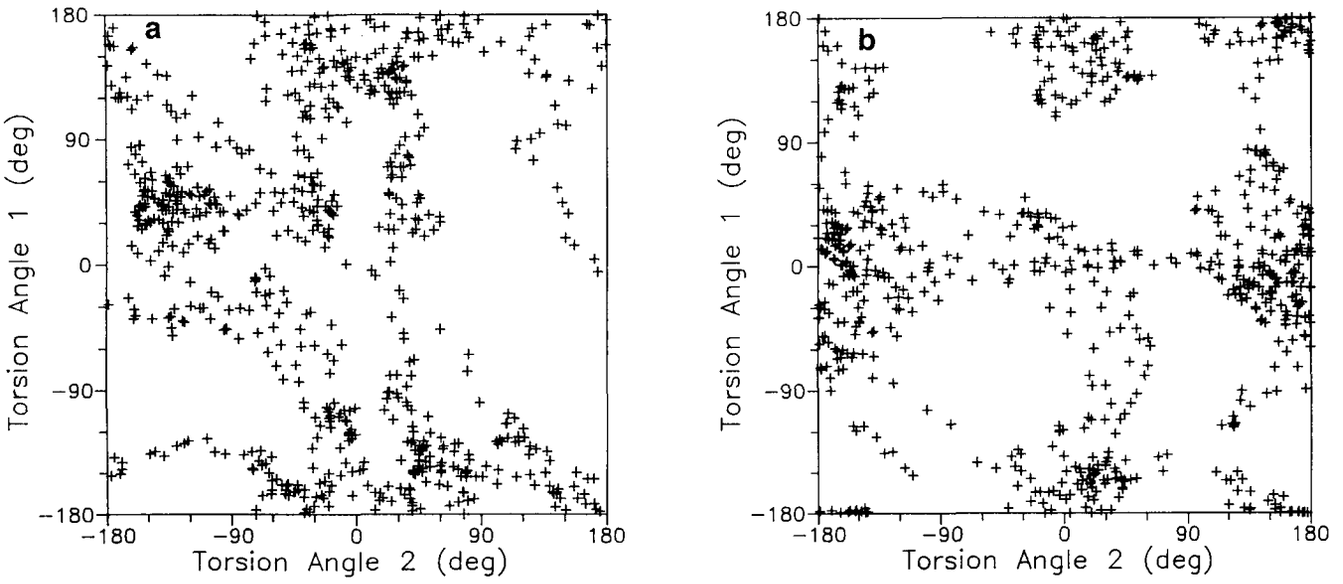

Figure 15 Torsion angle $\tau 1$ *versus* torsion angle $\tau 2$ for (a) PBZT and (b) PBO

value of this torsion angle. Beyond the initial 5000 fs where remnant warm-up effects could remain, there are few transitions through the coplanar conformations at 0 and 180°. This is surprising in view of the magnitude of the energy barriers, which are somewhat smaller than in PBO. The difference in behaviour can, in part, be attributed to the presence of hydrogens in the *ortho* positions on the phenyl rings, impediments to rotation which are obviously absent on the heterocyclic rings. Also contributing is the non-linearity developed by the isolated PPP molecules. This non-linearity combined with the presence of *ortho* hydrogens would certainly tend to make rotations through 0 and 180° difficult, more so than for a linear PPP molecule or even for a non-linear PBO or PBZT. The lack of coplanarity, then, may result indirectly from dealing only with an isolated PPP molecule, and molecules constrained to be straight, either artificially in a MD simulation or by neighbouring molecules in a crystal, may exhibit torsional behaviour quite different from that seen here. X-ray diffraction analyses[44,45], in fact, indicate that PPP oligomers in the solid state at room temperature adopt a coplanar arrangement of the rings. Intermolecular interactions must clearly play a significant role in determining the solid-state conformation, as has been demonstrated by recent calculations[45].

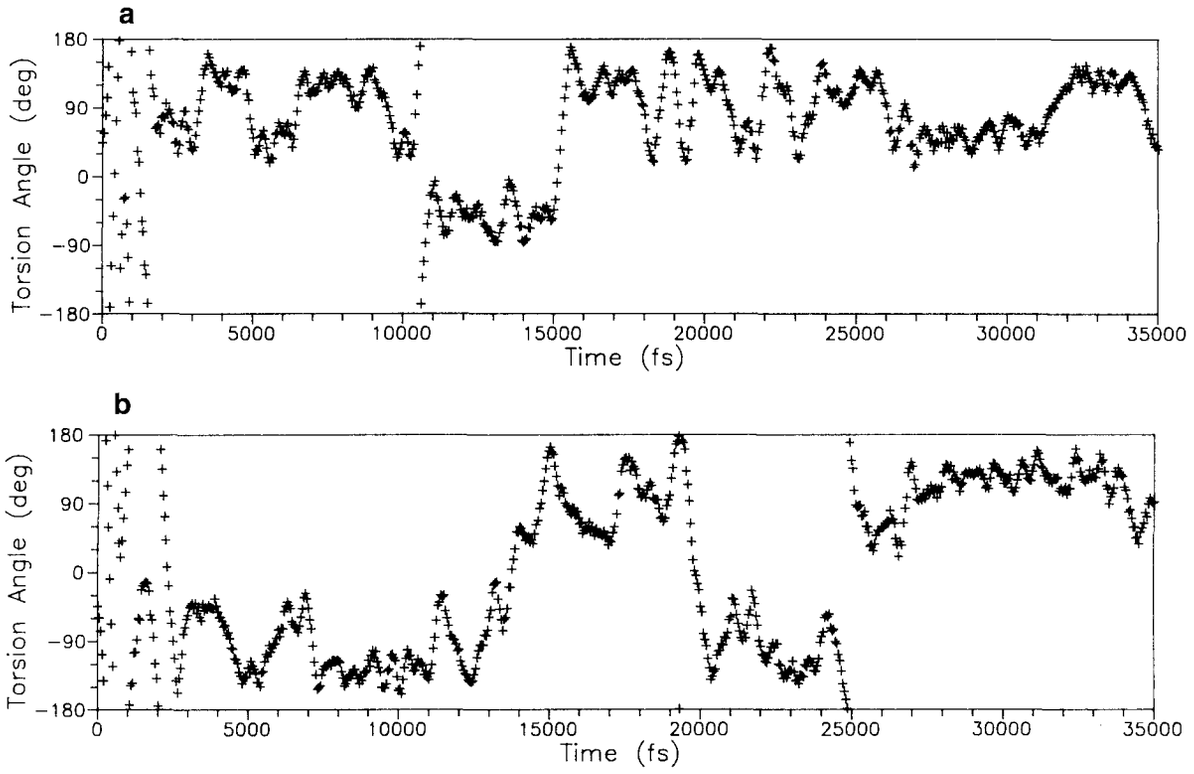

Figure 16 Torsion angles (a) $\tau 1$ and (b) $\tau 2$ *versus* time for PPP

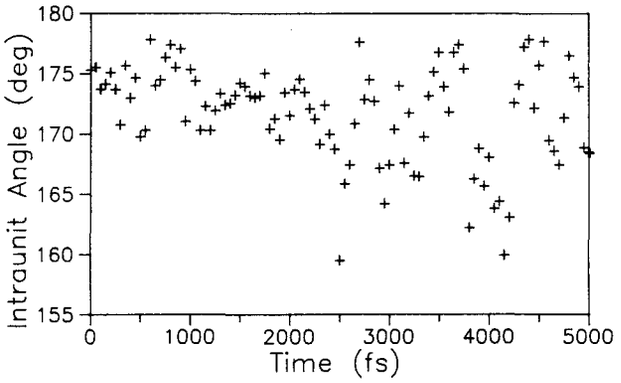

Figure 17 Intra-unit angle (EFG) *versus* time for PBZT

The angle EFG (see *Figure 3*) represents one of many possible measures of the linearity of a single repeat unit of the rigid rod materials. For a truly linear unit, the angle would have a value of 180°. The data for PBZT (*Figure 17*) for the first 5000 fs show that this angle varies over a 20° range. The striking periodicity of the distance plots is lacking, although remnant periodicity may be present. This appearance arises because the manner in which the angle is evaluated does not allow values > 180°. The effect is to fold the values which should be in the range 180–190° back onto the 170–180° range. Evaluation of this angle in a way which would carry with it the sense ('the sign') of the flexing would be advantageous, but is beyond the current capability of the software.

Less influenced by this folding is the angle between successive repeat units in the oligomer, angle CEG (DEG in PPP; see *Figure 3*). *Figure 18* shows this angle as a function of time for PBO, PBZT and PPP. All three materials show dramatic fluctuations within the time interval studied. PBO bends more than 40°, while PBZT and PPP bend up to 35° from linear. It is interesting to note that the magnitudes of these deflections are about the same as those observed in PBO high-resolution electron micrographs[17]. The high-frequency oscillations observed in the length *versus* time data are apparent in the PBO and PBZT data. PPP shows a more 'jumbled' appearance. This arises from the sampling interval (50 fs) being somewhat too large relative to the rate of change of the parameter being plotted. This probably occurs in the case of PPP because of the relatively shorter length of the repeat unit (4.3 Å for PPP compared with 12.0 Å for PBO or 12.3 Å for PBZT).

Persistence lengths

The persistent (or worm-like) chain model provides a convenient framework in which to analyse the overall behaviour of these molecular dynamics data. It also provides a means of comparing the flexibility observed here with experimental data on solution behaviour.

The inter-unit angles plotted in *Figure 18* provide one of the quantities needed to evaluate the persistence lengths of the rods. By the nature of the MD process used to generate them, the data are weighted in a statistical mechanical fashion. Thus, computing the average value of the cosine of the supplement of the inter-unit angle over the simulation time will give the properly weighted mean for $\Delta\psi$ describing the worm-like chain (see equation (2)). These values are presented in *Table 5*, as are the mean values of ψ, for PPP, PBO and PBZT. Combining these with the lengths of the repeat units (again the averaged value is used) gives the persistence lengths shown in the table. The number of repeat units represented by that calculated persistence length is also given. Though the PPP rod has the shortest persistence length in absolute terms, it is the stiffest rod

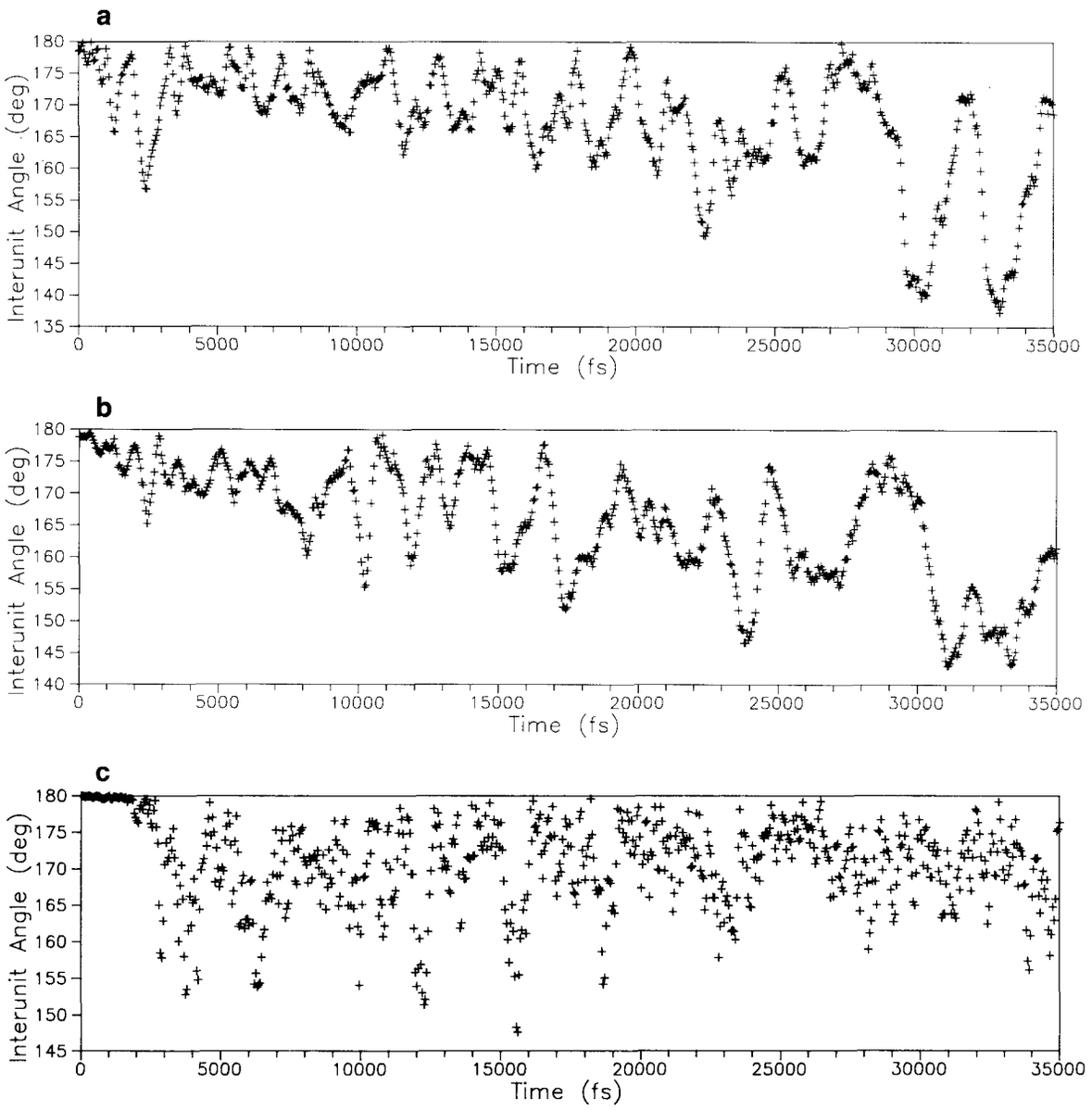

Figure 18 Inter-unit angle (CEG) *versus* time for (a) PBO, (b) PBZT and (c) PPP

Table 5 Calculated MD persistence lengths

Polymer	Segment length (Å)	$\langle\psi\rangle$ (deg)	$\langle\cos(\psi)\rangle$	Persistence length (Å)	Repeat units	Experimental (Å)
PPP	4.3	11.3	0.9807	220	51	–
PBO	12.0	13.1	0.9636	325	27	>640
PBZT	12.3	16.7	0.9448	215	17	>500

when the number of repeat units is considered. PBZT appears to be the least rigid of the molecules. This may be due, in part, to the lower torsion energy barriers compared with PBO and PPP.

Not surprisingly, the dynamic persistence lengths are much smaller than the static values (9000 and 3000 Å for PBO and PBZT, respectively). They are also smaller than experimental values (>500 Å and >640 Å for PBO and PBZT, respectively[14,15]). Considering the possible complications afforded by aggregation in solution, this too is not surprising. In addition, this analysis oversimplifies the complex atomic motions found in the dynamics runs and considers the deviations from linearity to be due only to a more global, simple bend type of deformation. Finally, solvent effects have not been considered. In particular, the effects of protonation of the rods in acid solvents might be expected to stiffen the rods. The effects of protonation on the out-of-plane bending and torsional force constants have been examined[46]. The results indicate that the barriers to rotation increase as charge is delocalized from the heterocyclic rings into the phenyl groups. The out-of-plane bending energy, on the other hand, remains nearly the same or decreases slightly.

In view of all these factors, the agreement between calculated and experimental data is acceptable and suggests that the behaviour observed in the MD simulations may indeed be representative of the motions that the molecules undergo in solution. Solvent effects may extend the time scale over which such motions occur because the solvent molecules must physically move (or be pushed) out of the way before the polymer can move. However, since there is likely to be little if any resistance to such solvent reorganization, and since even protonation does not appear to stiffen the polymer[46], the magnitudes of the deflections of the polymer from linearity may not be so different from those observed here.

Other calculations utilizing Rotational Isomeric State formalism in conjunction with parameters derived from MD simulations have also been reported[47]. The force field was selected explicitly because it gave the greatest resistance to bond angle deformations among the force fields considered. MD trajectories were computed for up to 1 ns. The resulting persistence lengths were comparable to the values observed experimentally.

Bending deformation energies

Central to the validity of the MD results is the ability of the molecular mechanics force field to mimic the behaviour of the real material. The force fields have generally been derived to give best agreement between theoretical and experimental (crystallographic) equilibrium geometries. Including vibrational frequency data among those that must be reproduced assures that the force field has reasonable derivatives with respect to the various molecular deformation (vibrational) modes. The out-of-plane bending properties, which so clearly play a major role in the deformations of the rigid polymers of interest here, have only a small role to play in most materials that have been studied by molecular mechanics techniques. It is likely, therefore, that there is less experimental foundation upon which those parameters are based.

To examine the validity of these force constants used to study PPP, PBO and PBZT, AM1 semiempirical molecular orbital calculations were undertaken. Molecules of biphenyl, phenyl benzobisthiazole, and phenyl benzobisoxazole (i.e. the relevant repeat units of the polymers) were constrained into bent geometries, as depicted in *Figure 12*. Except for the constraints necessary to keep the molecule bent, the energy was minimized with respect to all geometrical parameters. Bending constraints for PBO and PBZT were applied such that bending occurred either at the phenyl carbon or at the apex carbon of the heterocycle. For PBZT, bending at the heterocyclic carbon was induced in molecules having both 0 and 20° torsions about the inter-ring single bond. For biphenyl, the inter-ring torsion angle was initially 45° and for PBO, 0°. Both the original Tripos force field and the tailored force field with modified out-of-plane bending parameters were used to calculate the molecular mechanics energies for the starting and final (optimized) AM1 geometries. Since the results were qualitatively similar, data are presented only for the geometries resulting from the AM1 minimization.

Ab initio calculations were also made for biphenyl, using the Gaussian system of programs[48]. Calculations were made at the RHF/6-31G* level. The geometry was fully optimized, subject to the constraints required to impose the desired bending.

Figure 19 shows the relative energy *versus* bend angle for biphenyl. All energies are taken relative to the minimum value calculated by the same method. The AM1 results indicate the softest bending deformation. The *ab initio* results are quite similar to those using the original Tripos force field. [It should be remembered that the AM1 results also provide better agreement with experimental data (for the rotation barriers in biphenyl) than do the *ab initio* results.] Overall, this suggests the original Tripos force field is reasonably accurate or, if anything, errs by being too stiff rather than too flexible. The suggested[23] modifications to the out-of-plane bending parameters of the molecular mechanics force field appear to stiffen the rings too much in terms of this bending. Further refinement of the molecular mechanics force field using comparisons with AM1 and *ab initio* results of this type should be possible.

The interdependence of the bend angle and the minimum energy torsion angle was also investigated. For the AM1 and molecular mechanics optimizations of biphenyl, the starting torsion about the inter-ring single bond was 0°, such that for a zero bend angle, the rings were coplanar. This common starting point was chosen to avoid predisposing the results to a particular value. The starting point for *ab* initio calculations was a 40° torsion. The minimum energy torsion angles for the bent biphenyl molecules determined by the AM1 and *ab initio* methods were compared with the minimum energy values from molecular mechanics scans using 5° increments of the torsion angle. Both original and modified force fields indicate that the torsion angle increases by about 10° as the bend angle increases by 15°. The AM1 and *ab initio* results, on the other hand, indicate the torsion angle decreases by 5°. This difference in behaviour can probably be attributed to the fundamental difference in the methods. Molecular mechanics, which takes no account of delocalization, is dominated by steric interactions between the rings, while AM1 maintains the angle near 30° for the sake of delocalization, preferring to distort other bond angles (e.g. those governing the positions of the *ortho* hydrogens) instead. Note, also, that electrostatic effects were not considered in the molecular mechanics calculations, while they are included in the AM1 and

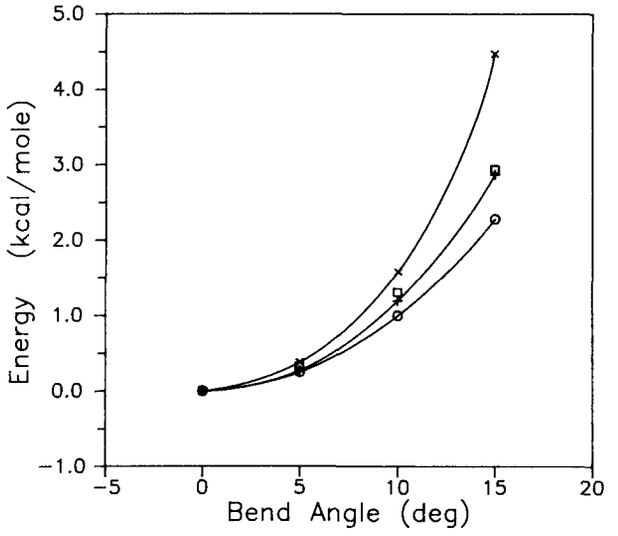

Figure 19 Relative energy *versus* bend angle for biphenyl calculated by AM1 (○), original out-of-plane bending parameters (+), modified out-of-plane bending parameters (×), and *ab initio* (□) methods

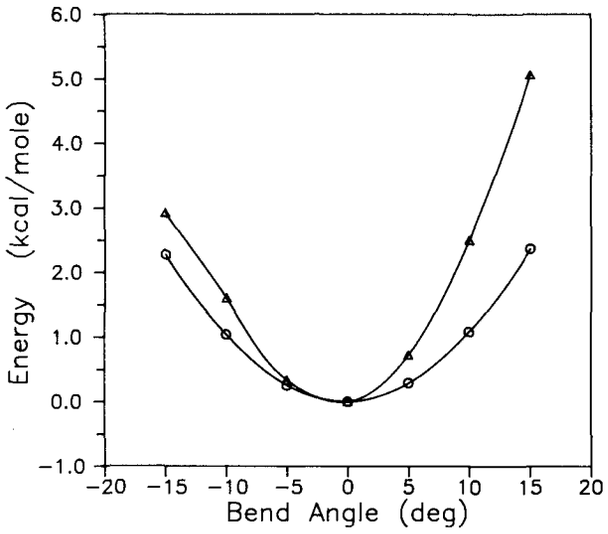

Figure 20 Relative energy *versus* bend angle for PBO calculated by AM1 (○) and molecular mechanics (△) methods. Negative angles correspond to bending at the phenyl carbon atom and positive angles correspond to bending at the heterocyclic carbon atom

ab initio calculations. Better agreement between the methods may be possible by further modification of the molecular mechanics force field.

Figure 20 shows the energies for PBO bent at the phenyl carbon (plotted at negative bend angles) and at the heterocycle carbon (plotted at positive bend angles). The AM1 energy increases slightly less rapidly when bending occurs at the phenyl carbon. However, this could be due to the manner in which constraints were applied. For bending at the phenyl carbon, only one internal coordinate needed to be constrained, while bending at the heterocyclic carbon required two internal coordinates to be constrained during the AM1 minimization. The molecular mechanics energies likewise increase more rapidly for bending at the heterocycle than at the phenyl carbon, and again more rapidly than do the AM1 values. The latter again indicates that the flexibility observed in the dynamics simulations is most probably a conservative representation of the real behaviour – if 'real' can be used to describe behaviour anticipated *in vacuo*.

Similarly, molecular mechanics and AM1 calculations were carried out for PBZT. For bending at the phenyl ring, the backbone torsion angle was adjusted during the minimization. For bending at the heterocyclic carbon, energies were calculated for torsion angles of 0 and 20°. AM1 energies increased less than molecular mechanics energies for a given bend angle. Both AM1 and molecular mechanics results indicate that the minimum energy torsion angle for the unbent molecule (20°) persists as the molecule is bent, and that the energy increase is less steep for this torsion angle than for a torsion of 0°. Bending at the heterocycle is somewhat more energetically favourable than bending at the phenyl ring.

Another approximation of the persistence length can be obtained by using the various energy *versus* bend curves. By fitting a polynomial to the data and using the resulting coefficients, the statistical mechanical average of the bend angle and its cosine can be evaluated. The values are given in *Table 6* for both AM1 and molecular mechanics energy curves. If the polymer repeat unit is taken as the length ΔL, the resulting persistence lengths (shown in the table) are too large. This underscores, especially, that the molecules must have multiple bend points per repeat unit, and cannot be considered to bend only at the apex carbon atoms. To achieve persistence lengths consistent with the experimental data, the ΔL values for PBO and PBZT would have to be of the order of 3 Å or less. Apparently, MD simulations may be necessary in order to obtain a realistic assessment of the flexibility of polymers whose spatial arrangement is not dominated by torsional rotations about single bonds.

CONCLUSIONS

The results of MD simulations of PBO, PBZT and PPP show the molecules to be surprisingly flexible in spite of their rod-like topologies. The soft deformation mode primarily responsible for this flexibility can be characterized as out-of-plane bending.

There remains much to study about the dynamics of the rigid rod molecules, with respect both to the methods and the materials. Even though the molecular architectures of the polymers are such that they have no bond rotations that can lead to conformational disorder, the kinetic energy at room temperature is sufficiently large that out-of-plane bending motions of the molecules allow remarkably large deviations of the trajectories from linearity. The results clearly indicate that out-of-plane bending provides unexpected flexibility to the polymer molecules. The force constants governing such deformation are critically important, and the validity of the results especially depend on their accuracy. A comparison of the results for out-of-plane bending deformation calculated by the molecular mechanics method (using the same force field as used in MD) and the semiempirical molecular orbital method (AM1) suggests that the MD results offer a conservative estimate of the molecular flexibility.

Regardless of the details of the molecular oscillations and larger scale bending, their dependence on chain length, or that solvent may damp the motions, the MD results point out that the molecular geometries of PBZT, PBO and PPP have an inherently soft deformation mode. The linear topology of the molecules has eliminated the usual torsional rotations and angle-bending deformations (compared with polyethylene, for instance) as a soft deformation mode for the polymer backbone, thereby increasing their tensile properties. However, their resistance to bending (in some preferred ways) remains relatively weak. Aggregation of several molecules would obviously form a stiffer structure than that offered by a single molecule, and bending and deformation of that structure would require cooperative deformation (bending) of its member molecules, but the individual molecules do not become stiffer[18]. Coupled with facile translation of one molecule past its neighbours, the underlying

Table 6 Persistence lengths from bending curves

Method	Polymer	$\langle\psi\rangle$	$\langle\cos\psi\rangle$	Persistence length (Å)
AM1	PPP	5.4	0.9956	980
	PBO	5.4	0.9956	2700
	PBZT	6.1	0.9944	2200
Molecular mechanics	PPP	4.6	0.9968	1300
	PBO	4.1	0.9974	4600
	PBZT	4.9	0.9963	3300

flexibility contributes to the diminished axial compressive properties observed in these materials. The results provide a basis for understanding the high-resolution electron microscopy results[17], where assemblages of molecules are seen to make substantial jogs and bends. While somewhat baffling if the rigid rod molecules are viewed as pencil-like, when the molecules are viewed as depicted in *Figure 11*, the molecular mechanism for such jogs is obvious.

The rigid rod polymers studied here do not behave as molecular pencils. The results suggest that any (essentially) one-dimensional structure will be subject to the same inherent weaknesses. Initial studies of two-dimensional molecules, ranging from polyacene to graphite-like sheet structures[49], suggest that these too have inherent flexibility. Thus, truly rigid molecular structures apparently must have some three-dimensional character. Polymers having structures based on cubane or adamantane, beside offering significant challenges to synthetic chemists, may be worthy goals on the way to achieving the ultimate in polymer mechanical properties.

REFERENCES

1 See, for example, *Macromolecules* 1981, **14**, 909–960, 1135–1138
2 Adams, W. W., Eby, R. K. and McLemore, D. E. (Eds) *Mater. Res. Soc. Symp. Proc.* 1989, **134**
3 Ulrich, D. R. *Polymer* 1987, **28**, 533
4 Wolfe, J. F., Loo, B. H., Sanderson, R. A. and Bitler, S. P. *Mater. Res. Soc. Symp. Proc.* 1988, **109**, 291
5 Prasad, P. N. *Soc. Photo-Optical Instrum. Eng.* 1986, **682**, 120
6 Rao, D. N., Swiatkiewicz, J., Chopra, P., Ghoshal, S. K. and Prasad, P. N. *Appl. Phys. Lett.* 1986, **48**, 1187
7 *Symp. J. Mater. Res. Soc. Meeting* 1988, Autumn (Abstract)
8 Prasad, P. N. *Mater. Res. Soc. Symp. Proc.* 1989, **134**, 635
9 Druy, M. A. and Domash, L. W. *Mater. Res. Soc. Symp. Proc.* 1989, **134**, 653
10 Allen, S. R., Filippov, A. G., Farris, R. J., Thomas, E. L., Wong, C.-P., Berry, G. C. and Chenevey, E. C. *Macromolecules* 1981, **14**, 1135
11 Choe, E. W. and Kim, S. N. *Macromolecules* 1981, **14**, 920
12 Adams, W. W. and Eby, R. K. *Mater. Res. Soc. Bull.* 1987, **12**, 22
13 Wierschke, S. G. *Mater. Res. Soc. Symp. Proc.* 1989, **134**, 313
14 Kumar, S. 'International Encyclopedia of Composites' (Ed. S. M. Lee), Vol. 4, VCH, New York, 1990, p. 51
15 Lee, C. C., Chu, S. G. and Berry, G. C. *J. Polym. Sci., Polym. Phys. Edn* 1983, **21**, 1573
16 Chu, S.-G., Venkatraman, S., Berry, G. C. and Einaga, Y. *Macromolecules* 1981, **14**, 939
17 Martin, D. C. and Thomas, E. L. *J. Mater. Sci.* 1991, **24**, 5171
18 Kluzinger, P. E., Green, K. A., Eby, R. K., Farmer, B. L., Adams, W. W. and Czornyj, G. *Soc. Plast. Eng. Tech. Papers* 1991, **37**, 1532
19 Burkert, U. and Allinger, N. L. *Am. Chem. Soc. Monogr.* 1982, **177**
20 McCammon, J. A. and Harvey, S. C. 'Dynamics of Proteins and Nucleic Acids', Cambridge University Press, 1987
21 Allen, M. P. and Tildesley, D. J. 'Computer Simulation of Liquids', Oxford University Press, 1987
22 Ciccotti, G., Frenkel, D. and McDonald, I. R. (Eds) 'Simulation of Liquids and Solids', North Holland Physics Publishing, 1987
23 Sybyl, Version 5.4, Tripos Associates, St Louis, MO, and related manuals
24 Clark, M., Cramer, R. D. III and Van Opdenbosch, N. *J. Comp. Chem.* 1989, **10**, 982
25 Fratini, A. V., Resch, T., Lenhert, P. G. and Adams, W. W. *Mater. Res. Soc. Symp. Proc.* 1989, **134**, 308
26 Wellman, M. W., Adams, W. W., Wolff, R. A., Dudis, D. S., Wiff, D. R. and Fratini, A. V. *Macromolecules* 1981, **14**, 935
27 Fratini, A. V., Cross, E. M., O'Brien, J. F. and Adams, W. W. *J. Macromol. Sci.-Phys.* 1985–86, **B24**, 159
28 Verlet, L. *Phys. Rev.* 1967, **159**, 98
29 Ryckaert, J. P., Ciccotti, G. and Berendsen, H. J. C. *J. Comp. Phys.* 1977, **23**, 327
30 Farmer, B. L., Wierschke, S. G. and Adams, W. W. *Polymer* 1990, **31**, 1637
31 Chem-X Molecular Modeling Software, Chemical Design Ltd, Oxford, UK
32 Dewar, M. J. S., Zoebisch, E. G., Healy, E. F. and Stewart, J. J. P. *J. Am. Chem. Soc.* 1985, **107**, 3902
33 Stewart, J. J. P. *MOPAC*, QCPE Program no. 455, Indiana University
34 Almenningen, A., Bastiansen, O., Fernholt, L., Cyvin, B. N., Cyvin, S. J. and Samdal, S. *J. Mol. Struct.* 1985, **128**, 59
35 Bastiansen, O. and Samdal, S. *J. Mol. Struct.* 1985, **128**, 115
36 Tsuzuki, S. and Tanabe, K. *J. Phys. Chem.* 1991, **95**, 139
37 Haaland, P. D., Pachter, R. and Adams, W. W. *J. Chem. Phys.* submitted
38 Jiang, H., Eby, R. K., Adams, W. W. and Lenhert, G. *Mater. Res. Soc. Symp. Proc.* 1989, **134**, 341
39 Tsvetkov, V. N. 'Rigid-Chain Polymers', Consultants Bureau, New York, 1989, p. 7
40 Freeman, J. J., Morgan, G. J. and Cullen, C. A. *Phys. Rev. B: Condens. Matter* 1987, **35**, 7627
41 Press, W. H., Flannery, B. P., Teukolsky, S. A. and Vetterling, W. T. 'Numerical Recipes', Cambridge University Press, 1986
42 Olson, H. F. 'Music, Physics and Engineering', Dover Publications, New York, 1967, p. 82
43 Dudis, D. S. and Connolly, J. W. personal communication
44 Delugeard, Y., Desuche, J. and Baudour, J. L. *Acta Cryst.* 1976, **B32**, 702
45 Baker, K. N., Fratini, A. V., Resch, T., Knachel, H. C., Adams, W. W., Socci, E. P. and Farmer, B. L. *Polymer* 1993, **34**, 1571
46 Farmer, B. L., Dudis, D. S. and Adams, W. W. in preparation
47 Zhang, R. and Mattice, W. L. *Macromolecules* 1992, **25**, 4937
48 Pople, J. A. *et al.* Gaussian 90, Revision F, Gaussian, Inc., Pittsburgh, 1990
49 Farmer, B. L., Dudis, D. S. and Adams, W. W. *Soc. Plast. Eng. Proc.* 1992, **2**, 1976